A Model for Volatiles Release into a Bubbling Fluidized-Bed Combustor

A volatiles release model has been developed to predict the location and quantity of coal volatiles that are released into a bubbling fluidized-bed combustor, using overbed, in-bed or underbed feed systems. This model not only considers time resolution of the simultaneous processes of coal devolatilization and coal particle movement after injection, but also takes account of the stochastic nature of this particle movement. Volatiles release is nonuniform, occurring throughout an industrial-scale bed, but only in restricted parts of a laboratory-scale bed. For the industrial-scale bed, 32% of volatiles are released directly into the freeboard while the particle is devolatilizing at the surface, whereas 24% are released there for the laboratory scale bed. The model predicts the formation of numerous discrete volatiles regions within the bed, in agreement with a new interpretation of experimental measurements from an in-bed oxygen probe. The model is shown to be consistent with other experimental in-bed measurements obtained during combustion of "simulated" volatiles.

John F. Stubington
Shu W. Chan
Stephen J. Clough
Department of Fuel Technology
School of Chemical Engineering and
Industrial Chemistry
University of New South Wales
Kensington, N.S.W. 2033, Australia

Introduction

The fluidized-bed combustion of volatiles is being studied since overbed burning of volatiles may result in higher freeboard temperatures. Secondary air may need to be injected above the bed to obtain complete combustion, and larger heat-transfer surface areas would be required for above-bed heat removal than for heat removed by in-bed tubes, for which the heat transfer coefficients are much higher. The objective of this work is to predict the in-bed volatiles combustion efficiency as a function of operating conditions and design parameters such as coal feed design, particularly with respect to feed point spacing for in-bed or underbed feeding. For this, a realistic understanding of the volatiles combustion process within the bed is needed. Before studying volatiles combustion, one first needs to know the details of the release of volatiles into the bed. This paper describes a model for predicting this volatiles release based on combinations of literature and experimental data on particle mixing and devolatilization rate.

Three different concepts for the release of volatiles into a fluidized-bed combustor have been proposed. The first is that the volatiles are released as a continuous fuel-rich region rising in plug flow through the bed as a "plume" (Bywater, 1980; Park et al., 1981). The second is that the volatiles form bubbles, which may separate from the coal particle (Yates et al., 1980) or remain attached to it (Pillai, 1981). However, Turnbull (1983) calculated that a 3-mm-diameter coal particle would generate a bubble of volatiles of about 120-mm in diameter and suggested that it would be impossible for such a bubble to remain with the coal particle. The third concept is that of a "volatiles evolution region," defined as being that part of the bed to which coal particles are mixed during devolatilization (Stubington, 1980). It should be noted that this "volatiles evolution region" is not the region of the bed occupied by volatiles, but the region of the bed within which volatiles are released from the devolatilizing particle. Some of this region will be occupied by oxygen-rich gases and some by volatiles.

Although earlier workers used simpler assumptions, Bywater (1980) and Stubington (1980) concluded that both devolatilization rate and solids circulation rate should be considered, because the two processes occur on the same time scale. The model of Bywater (1980) predicts a time-averaged volatiles release rate distribution throughout the bed by assuming a *constant* mean particle rise velocity. However, particle mixing is known to be a stochastic process caused by the passage of bubbles through the bed (Nienow and Chiba, 1985). The model presented here takes into account this stochastic nature of the particle mixing, as well as the time resolution of both devolatil-

Correspondence concerning this paper should be addressed to J. F. Stubington.

ization rate and particle movement during the devolatilization period.

The particle movement model described in this paper assumes that particle movement is caused solely by the bubbles and that a coal particle or any other large flotsam particle (Nienow et al., 1978) remains stationary in the bed until a bubble displaces it axially and radially to another stationary point higher up the bed. A fuel region forms from volatiles released while the particle is stationary, but it is detached from the particle when a bubble lifts the particle rapidly to another stationary point. This particle mixing process generates multiple discrete regions of volatiles within the bed as the particle rises to the bed surface. An injected coal particle reaches the bed surface before the release of all its volatiles, either directly from an above-bed feeder or by rising through the bed from an in-bed feeder. It remains at the bed surface, liberating some volatiles directly into the freeboard, until it moves to the wall and is carried back down into the bed by the general downward movement of inert bed particles. The particle then circulates to a particular depth of the bed, also releasing volatiles during its descent and stepwise ascent (as described above) until devolatilization is complete.

The size and location of these volatiles regions can be determined by simultaneously considering the movement and the devolatilization rate of the particle. The devolatilization of coal particles larger than 3 mm in diameter is dependent on several parameters including particle size, bed temperature, moisture content, and coal type (Stubington et al., 1987).

Calculations have been performed for a laboratory-scale reactor burning "simulated" coal particles (Stubington and Chan, 1986) to quantify the distribution of volatiles within and above the bed. Only 0.5 to 4.5% of the total volatiles were released into each of five volatiles fuel regions during the "simulated" coal particle's rise through the bed, a total of 24% of the volatiles were released directly into the freeboard and the remaining volatiles were released as the particle descended into the bed from the surface (43% during the first descent and 13% during the second descent). The volatiles release model has also been applied to an industrial-size combustor based on the dimensions and conditions given for the Tennessee Valley Authority 20-MW pilot-scale combustor (Bellgardt et al., 1987). A calculation of the volatiles distribution for "simulated" coal particles in the TVA combustor estimates that nine discrete volatiles regions would be formed as the particle rises to the surface with varying quantities of volatiles ranging from 0.5% to 12% of the total volatiles yield. Also, 32% of the total volatiles are calculated as being released directly into the freeboard while the particle is at the bed's surface.

The "volatiles evolution region" also differs for the two beds. For the low-velocity laboratory-scale combustor, volatiles evolution is restricted to a region rising from the in-bed feeder and a circulation region extending 0.12 m down from the bed surface, whereas volatiles are evolved nonuniformly throughout the bed of the industrial-scale combustor.

A new interpretation of in-bed oxygen probe signals is presented, which is consistent with the volatiles release model. The frequency distribution of oxygen partial pressure exhibits two peaks, typically at 10^{-1} atm and 10^{-13} atm. Experimental correlation has shown that these do *not* correspond to different oxygen concentrations in the bubble and particulate phases. Rather, the time variation of the oxygen probe signal is interpreted as detecting numerous discrete volatiles regions within the bed, in agreement with the volatiles release model. Statistical data determined from combined oxygen/bubble probe measurements within the bed during "simulated" volatiles combustion are also shown to be consistent with the volatiles release model presented.

This volatiles release model quantifies the interaction between devolatilization and particle mixing processes. It predicts the formation within the bed of multiple discrete volatiles-containing regions. The model also predicts, for specific operating conditions, the fractions of volatiles released within the bed and directly into the freeboard at the bed surface. Data from the model provide a starting point for consideration of volatiles combustion.

The model has been developed specifically for the bubbling bed regime of low-velocity fluidized-bed combustors. It may also be applied to circulating fluidized-bed combustors fed by large coal particles, which are not entrained (at their initial particle size) and therefore devolatilize in the dense bed at the base of the riser. It cannot be applied to volatiles release in the high-velocity riser of a circulating fluidized bed, since very little is known about particle mixing in this region; therefore, the model should not be used for circulating fluidized-bed combustors fed by small coal particles which devolatilize after elutriation from the dense bed.

Description of Coal Particle Movement

After a coal particle is introduced into a fluidized-bed combustor it will rise through the bed as a result of the bubbling action. The particle will effectively remain stationary until it is lifted by a bubble passing its vicinity. The particle is simultaneously displaced laterally and axially until it is shed from the bubble wake at another stationary point higher up in the bed. Since the velocity of the bubble is greater than the mean particle rise velocity, it is assumed that the particle rise between stationary points is instantaneous.

When a particle is injected through an in-bed pneumatic feeder (e.g., in our laboratory-scale reactor), it initially rises a short distance with a bubble from the injection air. It will then remain stationary for a period of time between bubbles which will be the inverse of the point bubble frequency at that position in the bed. The particle will then rise through a number of these stationary points in a stepwise manner until it reaches the bed surface.

At the bed surface the particle will be moved radially to the reactor wall by the action of erupting bubbles. Since particles from overbed feed systems will commence their movement at the bed surface, they will follow the same circulation pattern as for in-bed feed systems once the in-bed feed particles reach the bed surface for the first time. The downward flow of inert particles at the reactor wall will drag the particle down into the bed to a certain distance, before it will be picked up by a bubble and start to rise again in a stepwise movement. The particle will then circulate within this limited depth from the bed surface during and after its devolatilization.

Particle Mixing Data

The mean axial rise velocity of a submerged large flotsam particle has been determined experimentally by Nienow et al. (1978) using humidified air at room temperature for a variety of

bed materials of different density. They have developed the following dimensional relation between the mean rise velocity of a coal particle and the excess gas velocity:

$$\overline{U}_r = k(U - U_{mf})^{0.5} \tag{1}$$

where $k = 0.19$ for their experiments and where velocities are expressed in m/s. The mean particle rise velocity measured in our laboratory-scale combustor (described in the next section) was 0.17 m/s, considerably higher than the value of 0.06 m/s calculated from Eq. 1. This was attributed to the pneumatic in-bed feeding system increasing the local excess fluidizing gas velocity in the vicinity of the particles. Therefore, the value of k was modified to 0.51 to match the mean particle rise velocity measured in our laboratory-scale combustor.

Further work is necessary to determine the appropriate value (or correlation) for k in the TVA 20-MW combustor. However, in the absence of data which would allow estimation of the mean particle rise velocity in this bed, we have used $k = 0.19$ in Eq. 1 for modeling the TVA bed.

Although Eq. 1 gives the mean axial rise velocity of the coal particle, it does not define the periodic nature of the particle's upward motion. The particle will remain stationary at each position in the bed for the period of time between bubbles passing that position. Therefore, the stationary time is given by the inverse of the point bubble frequency. This frequency was measured in our experiments and the results agreed within 17% of the dimensional correlation of Cranfield and Geldart (1974):

$$f = 16.7\, h^{-0.72} \tag{2}$$

where h is the height above the distributor in cm, and f is the bubble frequency in Hz. The stationary time was calculated as the inverse of the point bubble frequency calculated from Eq. 2. Assuming instantaneous rise of the coal particle to the next stationary position, the distance risen by the particle was calculated as the stationary time multiplied by the mean axial rise velocity.

The first stationary time in our laboratory-scale combustor is a function of the flow rate of air through the in-bed pneumatic injector and was calculated using an expression for the bubble frequency in Hz from a submerged orifice given by Davidson and Harrison (1963):

$$f_i = \frac{g^{0.6}}{1.138\, G^{0.2}} \tag{3}$$

where G is the gas flow rate through the submerged orifice. It is assumed that the particle is stationary at the feed point, on average, for only half the bubble formation time, since the particle may be injected at any time between the start of formation of a bubble and its detachment from the injector. Therefore, the first stationary time is equal to half the inverse of the injector bubble frequency (f_i) from the submerged orifice given by Eq. 3. The second and subsequent stationary times were calculated using Eq. 2.

The mean radial displacement of a coal particle as it rises from one stationary point to the next within the bed can be estimated from the two-dimensional Einstein diffusion equation (Jost, 1952):

$$\overline{R^2} = 4D_{sr}\Delta t \tag{4}$$

In the first application of this method to coal particle diffusion in a fluidized-bed combustor (Stubington, 1980), the one-dimensional form of the Einstein diffusion equation was used by mistake (Einstein, 1905):

$$\overline{X^2} = 2D_{sr}\Delta t \tag{5}$$

The use of this equation was perpetuated in more recent articles (Lee et al., 1984; Zhang et al., 1987). However, lateral displacement of the coal particle in a fluidized-bed combustor can occur in two dimensions (r and θ or x and y), so Eq. 4 is the correct expression of the Einstein diffusion equation for this application.

It should be noted that the Einstein diffusion distance has been used only to estimate the mean radial displacement of a coal particle, using literature data on radial solids mixing which have been expressed as effective diffusion coefficients. This equation has *not* been applied to the radial gas-phase mixing between oxygen and volatiles required for combustion to occur.

Berruti et al. (1986) have developed a modified three-dimensional, empirical and dimensionless correlation, based on that proposed by Shi and Fan (1984) for estimating the solid radial dispersion coefficient D_{sr}. The data of Berruti et al. show that D_{sr} increases with height above the distributor and decreases near the wall of the reactor. Within the bed, the radial solids dispersion coefficient has therefore been calculated from the following correlation of Berruti et al.:

$$D_{sr} = 0.185\left[1 - \left(0.44 + 2.87\,\frac{h}{H_{mf}}\right)\left(\frac{r}{R}\right)^5\right](U - U_{mf})\, d_p\left[\frac{(U - U_{mf})d_p\rho_f}{\mu_f}\right]^{-0.25}\left[\frac{h}{d_p}\right]^{1.45}\left[\frac{\rho_s - \rho_f}{\rho_f}\right]^{-0.43} \tag{6}$$

A particle's lateral displacement at the bed surface caused by the eruption of a single bubble has been estimated from experimental observations in the laboratory-scale combustor. Experiments were undertaken with single particle injection to measure: first, the mean axial rise velocity discussed above; and secondly, the particle residence time at the bed surface before it was dragged down by the general downward velocity of sand near the wall of the combustor. The mean residence time of a particle at the bed surface was 2 seconds. The bubble frequency at the bed surface, calculated from Eq. 2, was 1.43 Hz; so, the particle would have been affected by approximately three bubbles during its movement from the center to the wall at the surface. If the particle is moved a mean distance, x, towards the wall by each bubble's eruption, then

$$x = Kd_b \tag{7}$$

assuming the distance moved is proportional to the bubble diameter. The measured bubble diameter at the surface was 0.064 m. Since three bubbles are required to move the particle a distance of 0.075 m (the radius of the combustor), K was calculated to be 0.4 for our experimental conditions.

The particle descending velocity was calculated from the rela-

tions given by Kunii and Levenspiel (1969)

$$U_d = \frac{\alpha\delta U_b}{1 - \delta - \alpha\delta} \tag{8}$$

where the parameters were estimated from the following equations:

$$\alpha = 0.2 \tag{9}$$

$$\delta = \frac{U - U_{mf}}{U_b + 2U_{mf}} \tag{10}$$

$$U_b = U - U_{mf} + U_{br} \tag{11}$$

$$U_{br} = 0.711(gd_b)^{0.5} \tag{12}$$

The bubble diameter in Eq. 12 was estimated from the correlation of Mori and Wen (1975) for the laboratory-scale combustor, since this correlation gave the closest agreement to bubble diameters measured from the bubble probe signal (Stubington and Chan, 1989). However, the correlation of Rowe (1976)

$$d_b = \frac{(U - U_{mf})^{0.5} h^{0.75}}{g^{0.25}} \tag{13}$$

was used to estimate the bubble diameter in Eq. 12 for the industrial-scale combustor, since Mori and Wen's correlation dealt specifically with bubbles whose growth was restricted by the walls of the reactor and such restriction would not be expected in the large cross-section of the industrial combustor.

The average depth of penetration of a large coal particle circulating in the bed was then determined from the correlation of Nienow et al. (1978):

$$d_{cir} = 1.2H_m(U - U_{mf})^{0.5} \tag{14}$$

This correlation gives the penetration depth for large flotsam particles which tend to segregate (such as coal) and predicts that the coal particles do not circulate all the way back down to the injector in the laboratory-scale bed.

Particle Movement Model Results

Laboratory-scale combustor

Preliminary volatiles combustion experiments have been performed in a laboratory-scale fluidized-bed combustor (Stubington and Chan, 1988a). The laboratory combustor was constructed from stainless steel, 150 mm ID × 600 mm high, and insulated with Kaowool. The fluidized bed was supported on a sintered stainless steel distributor plate, which was cooled by the fluidizing air supplied from a vortex blower. The bed consisted of sand particles with mean diameters of 550, 780, or 1,100 μm and was heated to operating temperature by a natural-gas-fired preheat burner exhausting into the side of the bed just above the distributor. When the bed achieved the steady-state operating conditions required, the gas and air supplies to the preheat burner were shut off and feeding of "simulated" coal particles (described in the next section) was started.

The feed rate of "simulated" coal particles was controlled by a variable speed drive attached to a rotating wheel with six

Table 1. Particle Heights, Stationary Times and Solid Radial Dispersion Coefficients for a Laboratory-Scale Fluidized Bed Combustor*

Position No.	Height Above Distributor (m)	Stationary Time (s)	Cumulative Time (s)	D_{sr} (m^2/s)
1	0.055	0.03	0.03	1.8×10^{-4}
2	0.060	0.22	0.25	2.1×10^{-4}
3	0.097	0.31	0.6	4.1×10^{-4}
4	0.149	0.42	0.8	7.7×10^{-4}
5	0.221	0.56	1.4	1.4×10^{-3}
6S	0.300	0.69	2.23	
7S	0.300	0.69	2.92	
8S	0.300	0.69	3.61	
9W	0.3–0.18	7.68	11.3	
10	0.262	0.63	11.9	
11S	0.300	0.69	12.6	
12S	0.300	0.69	13.3	
13S	0.300	0.69	14.0	
14W	0.3–0.18	7.68	21.7	
15	0.262	0.63	22.3	

*Experimental conditions: d_p = 0.78 mm; R = 0.075 m; U_{mf} = 0.205 m/s; H_{mf} = 0.26 m; H_m = 0.300 m; U = 0.315 m/s; T_b = 1,123 K; $\bar{U}_r$ = 0.17 m/s
S = particle at the bed surface
W = particle descending near the wall

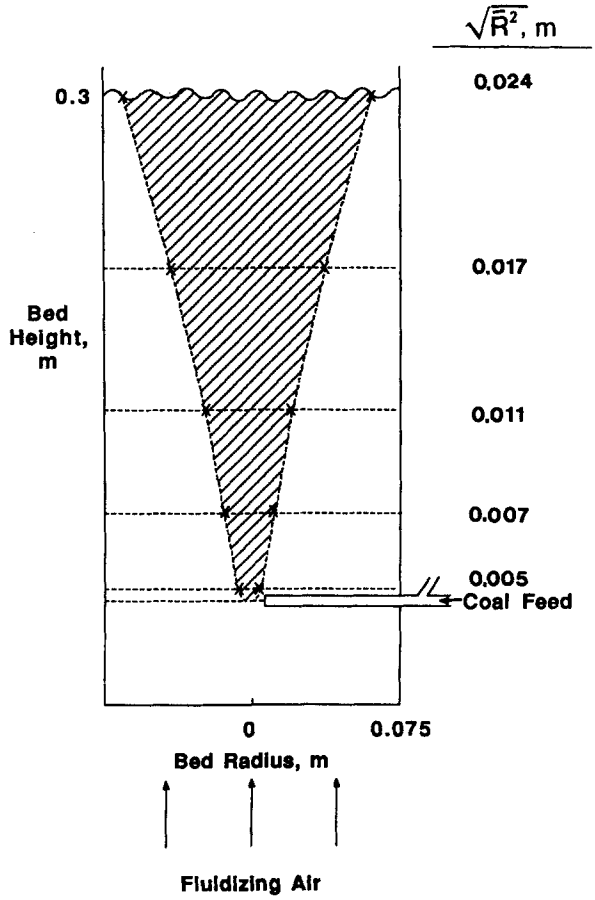

Figure 1. "Volatiles evolution region" for initial particle rise from in-bed feeder to bed surface for experimental conditions given in Table 1.
It shows five stationary particle axial positions and the root mean square radial displacement during particle rise to each position.

niches in its outer surface, each able to pick up a single "simulated" coal particle from an enclosed hopper. These particles were dropped down a tube to the particle injector. A small flow (20 L/min) of air was used to blow the particles into the bed through the injector, which projected 45 mm horizontally into the bed so that the particles were supplied approximately to the middle of the bed cross-section at a height 50 mm above the distributor. Sufficient particles could be stored in the hopper to fire the "simulated" particles for periods of 9–21 minutes, depending on the experimental conditions studied.

Most experiments were conducted at 850°C with an excess fluidizing velocity of 0.11 m/s and expanded bed height of 300 mm. Fuel/air ratio was varied from stoichiometric to 70% excess air.

The particle movement model quantified above was applied to the laboratory-scale fluidized-bed combustor, and the results in Table 1 show the particle heights, stationary times, and solid radial dispersion coefficients calculated for our laboratory-scale fluidized-bed combustor for the experimental conditions given.

The particles rise through the bed from a centrally-located in-bed injector within the shaded region depicted in Figure 1. This boundary marks the cumulative mean of displacements calculated using the two-dimensional Einstein diffusion equation (Eq. 4) with the solid radial dispersion coefficients calculated from Berruti et al.'s correlation (Eq. 6) and defines the "volatiles evolution region" for the initial particle rise from an in-bed feeder to the bed surface. This figure shows each of the five stationary levels through which the particle rises, as well as the mean radial displacement experienced during particle rise to each stationary position. It takes 1.5 seconds for the particle to rise to the bed surface from the particle injector, and a further 2 seconds to move to the wall of the laboratory-scale combustor at the bed surface.

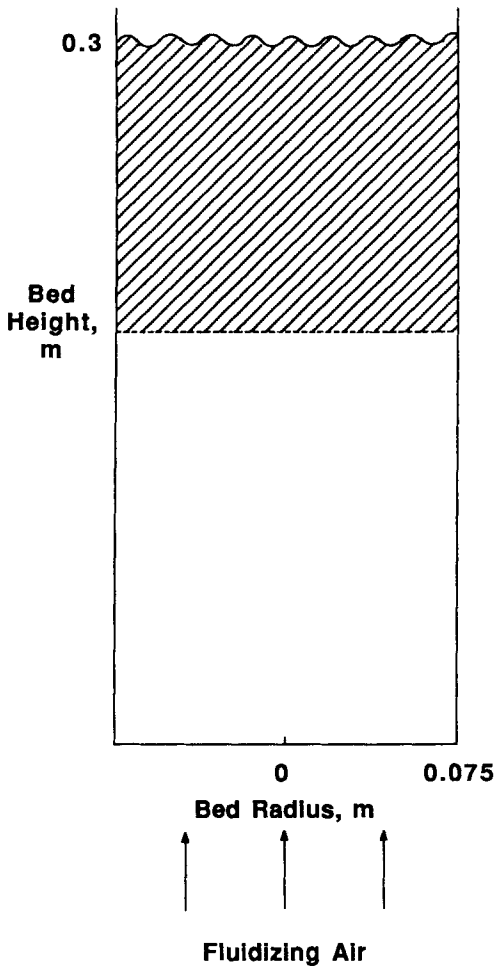

Figure 2. "Volatiles evolution region" during particle circulation down into the bed from bed surface for experimental conditions in Table 1.

The depth of particle circulation calculated from Eq. 13 was 0.12 m, and the corresponding "volatiles evolution region" is shown in Figure 2. This circulation region would be the same for an overbed feed system as well as an underbed feed system once the particles had reached the bed surface. It takes 7.7 seconds for the particle to descend to this depth and 0.6 second to rise back to the bed surface. The particle will continue to circulate within this region both during and after devolatilization.

Industrial-scale combustor

Table 2 shows the particle heights and stationary times that have been calculated for an industrial-scale fluidized-bed combustor based on the experimental conditions of the Tennessee Valley Authority 20-MW pilot-scale combustor using an underbed feed system.

The particle rises from the underbed injector through nine stationary positions before reaching the bed surface approximately 5 seconds after injection.

At the bed surface, the bubble diameter was 0.97 m from Eq.

Table 2. Particle Heights and Stationary Times in an Industrial-Scale Fluidized-Bed Combustor*

Position No.	Height Above Distributor (m)	Stationary Time (s)	Cumulative Time (s)
1	0.005	0.03	0.03
2	0.013	0.07	0.10
3	0.033	0.14	0.24
4	0.072	0.25	0.49
5	0.142	0.40	0.89
6	0.252	0.61	1.50
7	0.422	0.88	2.38
8	0.672	1.24	3.62
9	1.02	1.67	5.29
10S	1.26	1.53	6.82
11S	1.26	1.53	8.35
12S	1.26	1.53	9.88
13W	1.26–0.0	1.66	11.5
14	0.005	0.03	11.6
15	0.013	0.07	11.7
16	0.033	0.14	11.8
17	0.072	0.25	12.1
18	0.142	0.40	12.5
19	0.252	0.61	13.1
20	0.422	0.88	14.0
21	0.672	1.24	15.2
22	1.02	1.67	16.9
23S	1.26	1.53	18.4
24S	1.26	1.53	19.9
25S	1.26	1.53	21.5
26W	1.26–0.0	1.66	23.2

*Experimental conditions: d_p = 1.02 mm; R = 0.915 m; U_{mf} = 0.32 m/s; H_m = 1.26 m; U = 2.42 m/s; T_b = 1,107 K; $\bar{U}_r$ = 0.28 m/s
S = particle at the bed surface
W = particle descending near the wall or between particle feeders

13. Assuming that the constant in Eq. 7 is the same as for the laboratory-scale reactor, $K = 0.4$, the mean distance moved towards the wall by the particle at the bed surface is 0.39 m for each erupting bubble. Given that the equivalent bed radius is 0.915 m and the bubble frequency at the surface is 0.513 Hz, 2.4 bubbles would be required to move the particle from the center of the surface to the downward circulation region between feeder points or at the wall. The time taken for this traverse is 4.6 seconds. The particle descends right to the bottom of the industrial-scale bed in 1.7 seconds, in contrast to the 7.7 seconds required for it to descend only 0.12 m in the laboratory-scale reactor. This is principally because of the much higher superficial fluidizing gas velocity used in the larger combustor. The particle then begins its second circulation rising from the base of the combustor, since the circulation depth is equal to the bed height.

Coal Particle Devolatilization

The experimental study of the combustion of coal volatiles in a fluidized bed is complicated by the simultaneous combustion of the char from particles which have already devolatilized. In order to eliminate char combustion, a "simulated" coal particle was developed by Stubington and Chan (1986). The "simulated" coal is a 6.5-mm-diameter alumina catalyst particle, which has been vacuum-impregnated with a heavy paraffinic base oil to match the volatiles yield and the devolatilization time of a similarly sized coal particle. Once the volatiles are evolved from the "simulated" coal particle, an inert sphere of alumina remains as the residue instead of a reactive char particle. Figure 3 shows the plot of cumulative percent yield of volatiles vs. time for a "simulated" coal particle injected into a fluidized bed at 1,123 K under nitrogen, and this curve has been used as a typical devolatilization profile for the volatiles release modeling.

This devolatilization profile was measured in a small stainless steel reactor (35 mm diameter × 200 mm high) containing an 80-mm-deep bed of sand (500–599 μm) supported on a perforated stainless steel distributor and fluidized by preheated nitrogen at 1.5 times the measured minimum fluidizing velocity. Single impregnated particles were dropped into the bed for varying times, retrieved in a wire basket, quenched in dry ice, and weighed to determine volatiles loss. The devolatilization rate of a coal particle is affected by several parameters including particle size, bed temperature, moisture content, and coal type (Stubington et al., 1987). We have chosen to use the experimentally-determined devolatilization rate profile, in the absence of a reliable model which takes account of all of these parameters. Once a reliable devolatilization model becomes available, it could easily be incorporated into our volatiles release model.

Volatiles Release Model

The quantities and locations of volatiles released into the bed are determined by combining the results of the particle movement model with the time-resolved devolatilization profile. During each stationary period of the particle, volatiles are released from the particle into the bed to form a discrete volatiles region. When the particle is moved by a bubble, the particle detaches from this volatiles region and starts forming a new volatiles region at its next stationary position. Thus, a number of discrete volatiles regions are formed during the particle's rise to the bed surface, corresponding to the number of stationary positions of the particle during this rise. While the particle is at the bed surface, volatiles are evolved directly into the freeboard so that their combustion may not provide heat energy directly to the bed.

The particle movement model results for the laboratory-scale combustor have been superimposed on the time-resolved devolatilization profile for the "simulated" coal particle in Figure 3 The cross-hatched areas mark the times that the particle is at the bed surface. As the particle first rises to the bed surface from the in-bed feeder, 17% of the volatiles are released as five discrete volatiles regions containing the following consecutive yields of volatiles: 0.5%, 3.5%, 4.5%, 4.0%, and 4.5%. Approximately 17% of the volatiles are then released at the bed surface (i.e., into the freeboard) as the particle moves to the wall. Dur-

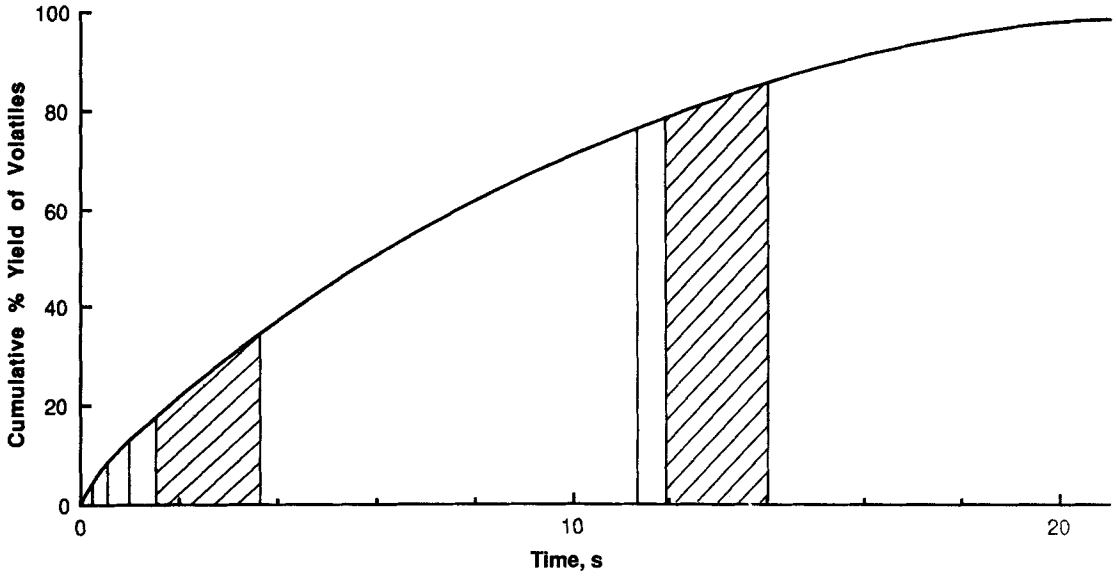

Figure 3. Combination of time-resolved volatiles yield and particle movement after injection.
It predicts locations and quantities of volatiles release for experimental conditions in Table 1.

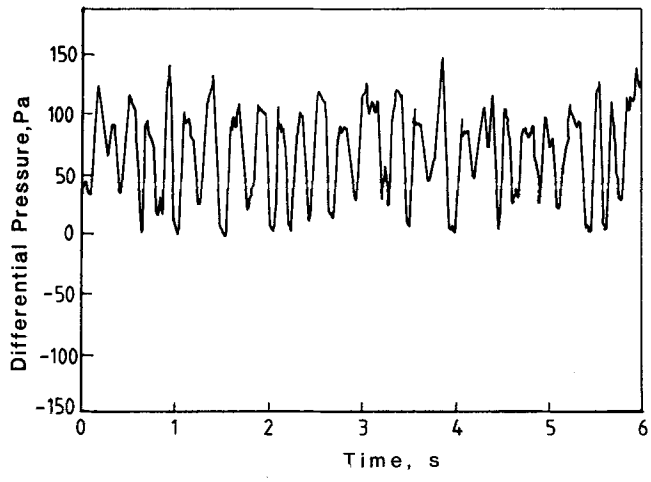

Figure 4. Typical bubble probe signal from the combined probe during combustion of "simulated" coal particles in the laboratory combustor.
Experimental conditions are given in Table 1.

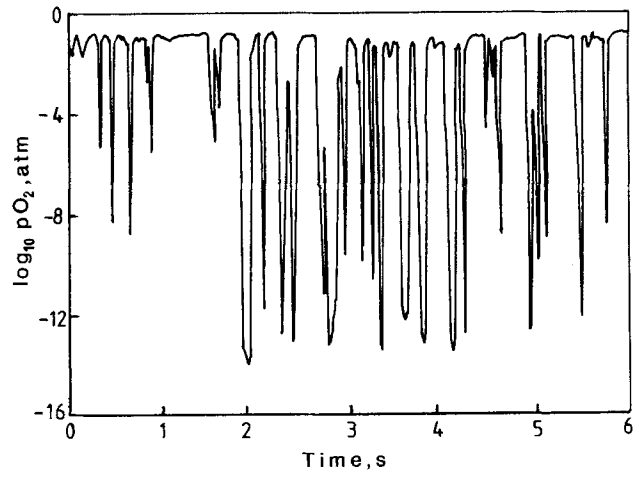

Figure 5. Typical oxygen partial pressure variation with time from the combined probe during combustion of "simulated" coal particles in the laboratory combustor.
Experimental conditions are given in Table 1.

ing the first particle descent, 43% of the volatiles are released into the bed, followed by another 3% during the particle rise to the bed surface from its circulation depth of 0.12 m.

A further 7% of volatiles are released into the freeboard when the particle is at the surface for the second time, and the balance of the volatiles are released during the second downward movement of the particle.

The particle movement times, calculated from our model, for the TVA combustor have also been combined with the volatile yield vs. time curve for the "simulated" coal particle. The "simulated" coal particle would devolatilize during its first two circulations within the bed. Approximately 45% of the volatiles would be released during the initial particle rise from the underbed feeder to the surface, as nine discrete volatiles regions within the bed with amounts ranging from 0.5% to 12% of the total volatiles are released. The next 25% of the volatiles would then be released directly into the freeboard as the particle was moved to the wall by erupting bubbles at the bed surface. As the particle descends to the base of the bed, another 7% of the volatiles would be released, followed by a further 15% during the particle's second rise to the surface. The balance (7%) of the volatiles would be evolved during the second sojourn of the particle at the bed surface. The volatiles release model is therefore consistent with visual observations of devolatilizing coal particles at the bed surface (Atimtay, 1980; Pillai, 1982), since it predicts a significant fraction of volatiles release at the surface (24% for the laboratory-scale and 32% for the industrial-scale combustor).

Interpretation of Oxygen Probe Signal

The formation of a large number of discrete volatile-containing regions within the bed suggests a new way of interpreting the signals from in-bed oxygen probes. Figure 5 shows a typical response from our in-bed oxygen probe during combustion of "simulated" coal particles in our laboratory fluidized-bed combustor (Stubington and Chan, 1988a). We believe these signals indicate the presence of numerous discrete volatiles regions within the bed, in agreement with the volatiles release model presented above. Before discussing our experimental evidence in support of this interpretation, the probe, the data obtained from it, and earlier interpretations are discussed briefly.

A combined oxygen/bubble probe was developed (Stubington and Chan, 1989) to simultaneously monitor oxygen partial pressure and detect bubbles at the probe tip, for studying the combustion process of volatiles within the bed. Oxygen partial pressure was measured *in situ* by a stabilized-zirconia solid electrolyte pellet, supported in the end of an alumina tube with porous platinum electrodes on the inner and outer surfaces of the pellet. Air was supplied to the inner electrode, as the reference gas and oxygen partial pressure at the outer electrode was calculated from the EMF (electromotive force) developed between the electrodes using the Nernst equation:

$$E = \frac{RT}{4F} \ln\left[\frac{p_i}{p_o}\right] \tag{15}$$

The presence of a bubble at the oxygen sensor was detected by measuring the differential pressure between two pressure probes located vertically below and above the oxygen sensor. The pressure probes consisted of 3.2-mm-OD stainless steel tubes attached to the alumina tube supporting the oxygen sensor. The probe tips were flattened to prevent blockage by the sand particles and were separated vertically by 9 mm. Whenever the combined probe was surrounded by particulate phase, the differential pressure transducer connected between the pressure probes detected the average pressure gradient in the bed; however, when a bubble enveloped the end of the combined probe, the differential pressure dropped to zero. First-order time constants for the responses of the probe were 0.02 s for the oxygen probe and 0.01 s for the bubble probe, and the signals were recorded simultaneously on an HP 7090 A measurement/plotting system at a sampling rate of 167 Hz.

"Simulated" coal particles were burnt in the laboratory fluidized-bed combustor to remove the complication of simultaneous char combustion in the bed, ensuring that measurements from the oxygen probe were attributed unequivocally to volatiles combustion. Walsh et al. (1986) suggested that coal volatiles

were cracked on the surfaces of the bed particles, depositing carbon on these particles and that this pyrolysis was enhanced by the catalytic effect of calcium oxide when limestone was used as the bed material. In our experiments, such secondary reactions on the bed particle were minimized by using: (i) sand as the inert bed material and (ii) a paraffinic hydrocarbon for the "simulated" volatiles.

Minimising these reactions kept more of the volatiles in the gaseous phase and allowed us to determine the phase location of volatiles and oxygen from the combined probe.

Figures 4–7 present data obtained from the combined probe, located centrally in the bed at a height of 250 mm above the feed level, when the fuel/air ratio was stoichiometric. Figures 4 and 5 illustrate the corresponding raw signals from the bubble and oxygen sensors, respectively; Figure 6 gives the frequency distribution of oxygen partial pressures for the 24 s of data obtained at this location; and Figure 7 gives the cross-correlation function between oxygen and bubble signals for these same data.

Similar in-bed oxygen probe signals have been obtained during coal combustion in fluidized-bed combustors, and two alternative interpretations have been suggested. The first interpretation was that the oxygen concentration was different in each of the two phases (bubble and particulate) within the bed (Holt et al., 1982; Saari and Davini, 1982; Li et al., 1984; Ljungström, 1985; Minchener et al., 1985).

These workers suggested that the peaks in the frequency distribution of oxygen partial pressure, observed at 10^{-1} and 10^{-13} atm in Figure 6, indicated different mean oxygen concentrations in the particulate and bubble phases. However, the low values (<0.3) of the cross-correlation coefficient in Figure 7 show that there was no significant correlation between the oxygen and bubble signals. Closer examination of the corresponding signals from bubble and oxygen sensors revealed occasional transitions from low to high pO_2 occurring within a bubble. Therefore, the fluctuating oxygen concentration within our bed does *not* occur as a result of differences in oxygen concentration between the bubble and particulate phases.

The second interpretation (de Kok et al., 1985) was to provide support for the diffusion flame (Stubington and Davidson, 1981) or plume (Park et al., 1981) model of volatiles combustion, by considering the fraction of time substoichiometric conditions prevailed at different radial positions. The meandering plume model was first proposed by Jovanovic et al. (1980) to explain the instantaneous tracer concentration fluctuations measured when tracer gas was injected continuously into a two-dimensional fluidized bed through a line source above the distributor plate. When this tracer concentration vs. time data are compared with our oxygen concentration fluctuations (Figure 5), the oxygen partial pressure is seen to fluctuate more rapidly and much more often than the tracer gas concentration, suggesting that our oxygen concentration fluctuations cannot be explained by the meandering plume model, since the meandering plume model does not account for the extremely short time scale of observed oxygen fluctuations.

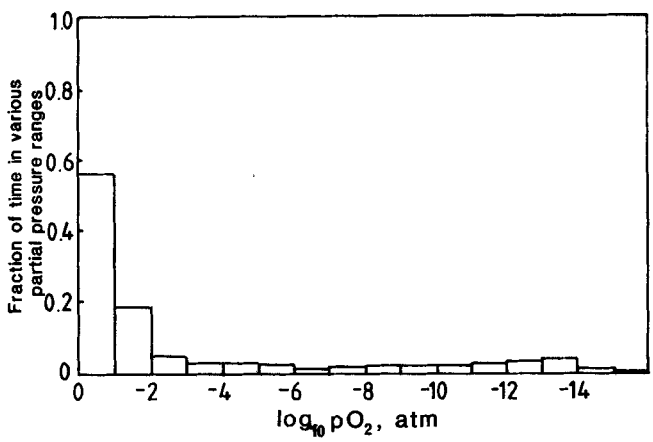

Figure 6. Frequency distribution of oxygen partial pressures during combustion of "simulated" coal particles in the laboratory combustor.
Experimental conditions are given in Table 1.

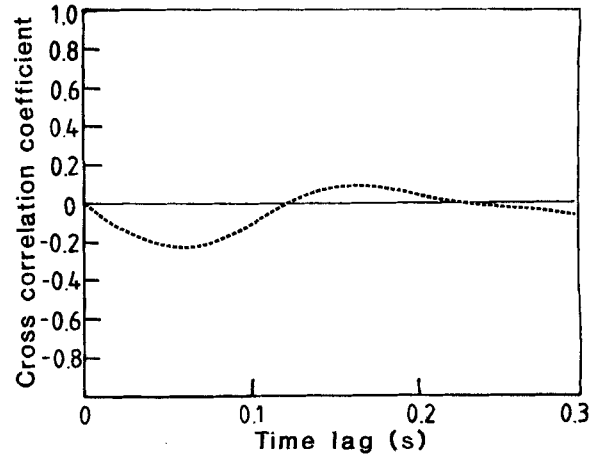

Figure 7. Cross-correlation coefficient between oxygen and bubble sensors.
Experimental conditions are given in Table 1.

Average *vertical* sizes of the observed regions of low oxygen concentration were calculated to range from 55 to 83 mm for the conditions of Figure 5, depending on position in the bed (Stubington and Chan, 1988b). We do not believe these indicate a single volatiles plume moving extremely rapidly around the bed, but interpret our data as measurements of numerous discrete volatiles regions within the bed.

No CO/CO_2 measurements could be made *in situ* to distinguish between unburnt volatiles and combustion products. However, some combined probe data were obtained while firing the preheat gas burner into the bed. The preheat burner was fed with air and LPG so that combustion was almost complete before the gases were exhausted into the bed. (The preheat burner flame projected only 75 mm into the empty combustor.) The oxygen probe response when firing the preheat burner alone into the laboratory fluidized bed is shown in Figure 8. This figure shows that combustion products alone generate pO_2 levels down to only 10^{-5} atm, suggesting that pO_2 levels below 10^{-10} atm do indicate the presence of unburnt volatiles (Stubington and Chan, 1989).

Further experimental evidence to support the interpretation of low pO_2 levels as regions containing unburnt volatiles was obtained from visual observations of the top surface of the bed, during combustion of the "simulated" coal volatiles. Numerous, small, discrete, orange-yellow diffusion flames were observed immediately above the bed surface. These flames indicated that unburnt volatiles were escaping from the top of the bed, and

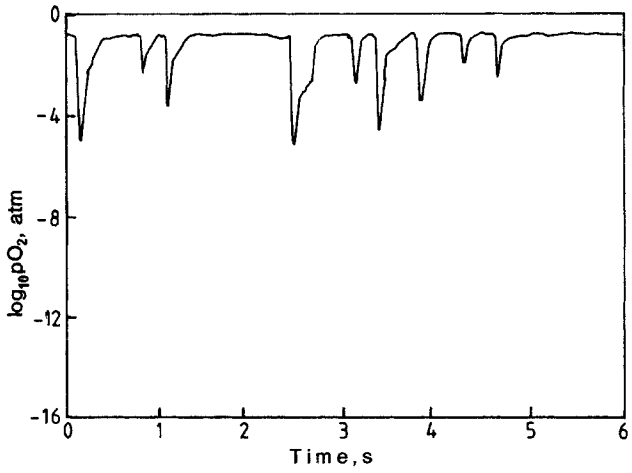

Figure 8. Oxygen probe signal for combustion products from preheat gas burner only.

therefore the in-bed probe should have been immersed in unburnt volatiles for some of the time. Furthermore, a single continuous flame was not observed moving around the bed surface, as would be predicted by the plume model; rather, a large number of separate flames were observed at any one time, each being quickly extinguished. These observations strongly support the contention that the bed contained numerous distinct volatiles-containing regions, which burnt via a diffusion flame at their boundaries.

Other Experimental Observations

Extensive experimental data have been obtained from the combined oxygen/bubble probe during combustion of the "simulated" coal particles in the laboratory fluidized-bed combustor (Stubington and Chan, 1988b). The data reported here for comparison with the volatiles release model were obtained at the stoichiometric ratio of volatiles fed in the "simulated" coal particles to oxygen supplied in the fluidizing air. The fraction of time spent by the probe in volatile-rich regions (i.e., $pO_2 < 10^{-10}$ atm) was determined from the oxygen signal at various positions in the bed. Figures 9 and 10 show the data for bed heights of 300 and 410 mm, respectively. This fraction was quite low (<0.3) for all conditions studied. The higher fraction of volatiles observed just below the surface of the bed supports the picture of the volatiles region shown in Figure 2. Further support for this picture is found by considering the effect of bed height on the fraction of

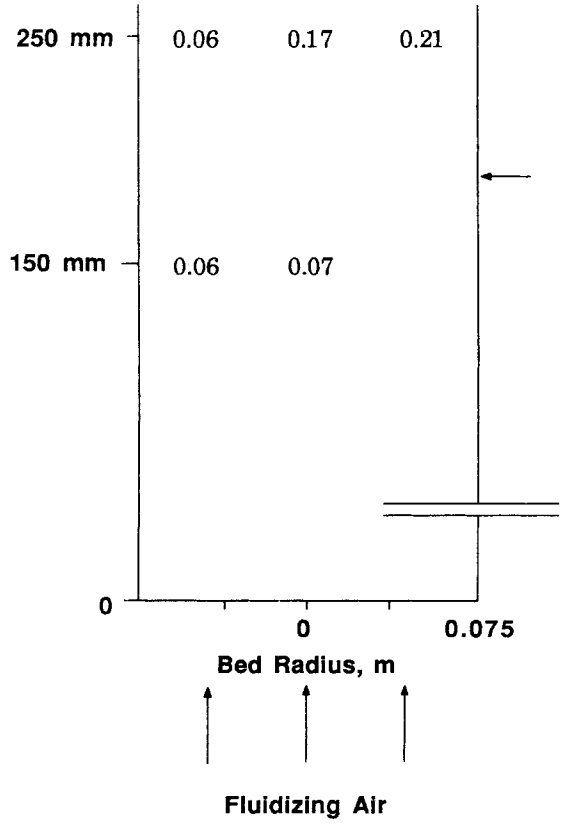

Figure 9. Fraction of time in volatile-rich regions at various positions in the bed for a bed height of 300 mm.
Experimental conditions are given in Table 1.

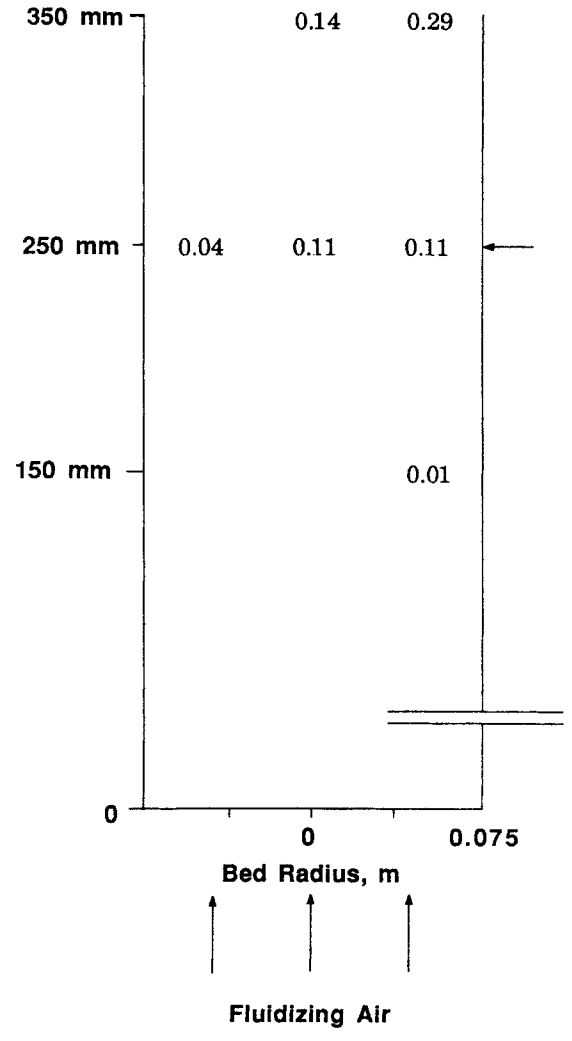

Figure 10. Fraction of time in volatile-rich regions at various positions in the bed for a bed height of 410 mm.
Experimental conditions are given in Table 1.

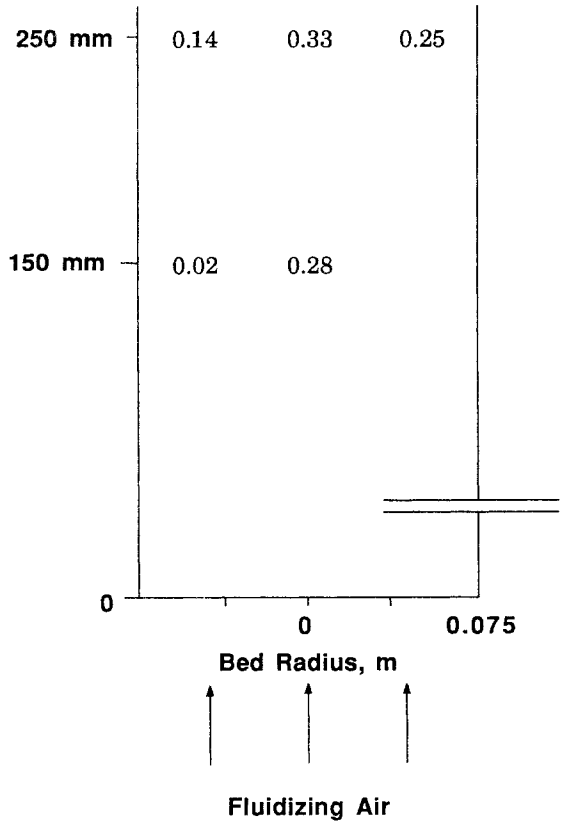

Figure 11. Fraction of volatile-rich time in bubble phase.
Experimental conditions are given in Table 1.

time in volatile-rich regions. The circulation depths estimated from Eq. 13 are indicated by the arrows on the right side of Figures 9 and 10. The increase in bed height from 300 to 410 mm significantly reduced the fraction of time in volatile-rich regions at a height of 250 mm above the distributor, since this level has moved down to the base of the recirculation zone at the top of the bed.

Whether the volatiles are released into the bubble phase or the particulate phase depends on the location of the devolatilizing particle. Our model assumes instantaneous rise of the particle with a bubble so that volatiles are released while the particle is stationary in the particulate phase. However, we are not concerned about the phase location of volatiles release for *industrial fluidized-bed combustors,* since they usually operate in the cloudless bubble (La Nauze, 1985) or "straight-through flow" regime. In this regime, volatiles released from a devolatilizing particle (in either phase) would rise up through the bed with the general upward gas flow, passing through both bubbles and particulate phase in their path. This rapid flow of gas through the bubbles explains why there is no correlation between oxygen concentration and phase location from our combined probe data. This physical picture is consistent with observations from the combined oxygen/bubble probe (Stubington and Chan, 1988a) that volatiles regions are usually observed in the particulate phase, but sometimes occupying part or all of a bubble and the adjacent particulate phase. The combined probe results were analyzed to determine the fraction of the total volatiles-rich time which occurred in the bubble phase, and Figure 11 illustrates the distribution of this statistic throughout the bed for the conditions of Table 1. The low values of this fraction show that the majority of the volatiles are detected within the particulate phase, in qualitative agreement with the volatiles release model.

Acknowledgment

The authors gratefully acknowledge the financial support for this project provided under the National Energy Research Development and Demonstration Program, Project No. 786, which is administered by the Australian Commonwealth Department of Primary Industries and Energy.

The Combustion Laboratory of Pennsylvania State University is also gratefully acknowledged for their assistance in preparing this manuscript.

Notation

d_b = bubble diameter, m
d_p = particle diameter, m
d_{cir} = circulation depth from the bed surface, m
D_{sr} = lateral dispersion coefficient of solids, m^2/s
f = bubble frequency, Hz
f_i = injector bubble frequency, Hz
g = acceleration due to gravity, m/s^2
G = gas flow rate through a submerged orifice, m^2/s
h = height above the distributor, m
H_m = maximum bed height, m
H_{mf} = bed height at minimum fluidizing conditions, m
k = constant in Eq. 1
K = constant in Eq. 7
pO_2 = oxygen partial pressure, atm
r = radius from the bed center, m
R = bed radius, m
$\overline{R^2}$ = mean square displacement for 2-D dispersion, m^2
t = time, s
T_b = bed temperature, K
U = superficial fluidizing velocity, m/s
U_b = velocity of a bubble rising through the bed, m/s
U_{br} = velocity of a bubble with respect to the emulsion phase, m/s
U_d = particle descending velocity, m/s
U_{mf} = minimum fluidizing velocity, m/s
$\overline{U_r}$ = mean particle rise velocity, m/s
x = mean radial displacement of particle towards the wall at the bed surface, m
$\overline{X^2}$ = mean square displacement for 1-D dispersion, m^2

Greek letters

α = ratio of wake volume to bubble volume
Δt = time increment, s
δ = fraction of fluidized bed consisting of bubbles
μ_f = fluid viscosity, $kg \cdot m^{-1} \cdot s^{-1}$
ρ_f = fluid density, kg/m^3
ρ_s = solid density, kg/m^3

Literature Cited

Atimtay, A., "Combustion of Volatile Matter in Fluidized Beds," *Fluidization,* G. R. Grace and J. M. Matsen, eds., Plenum, New York, 159 (1980).

Bellgardt, D., M. Schoessler, and T. Werther, "Lateral Nonuniformities of Solids and Gas Concentrations in Fluidized-Bed Reactors," *Powder Technol.,* **53,** 205 (1987).

Berruti, F., D. S. Scott, and E. Rhodes, "Measuring and Modelling Lateral Solid Mixing in a Gas-Solid Fluidized-Bed Reactor," *Can. J. Chem. Eng.,* **64,** 48 (1986).

Burke, S. P., and T. E. W. Schumann, "Diffusion Flames," *Ind. Eng. Chem.,* **20**(10), 1000 (1928).

Bywater, R. J., "The Effects of Devolatilization Kinetics on the Injector Region of Fluidized Beds," *Int. Conf. Fluidized Bed Combustion,* Atlanta, Vol. III, 1092 (1980).

Cranfield, R. R., and D. Geldart, "Large Particle Fluidization," *Chem. Eng. Sci.,* **29,** 935 (1974).

Davidson, J. F., and D. Harrison, *Fluidized Particles,* Cambridge University Press, Cambridge (1963).

De Kok, J. J., M. W. C. M. A. Nieuwesteeg, and W. P. M. van Swaaji, "An Experimental Evaluation of the Plume Model for Atmospheric Fluidized-Bed (Coal) Combustors," *Int. Conf. on Fluidized Bed Combustion*, ASME, 105 (1985).

Einstein, A., Über die von der Molekularkinetischen Theorie der Wärme Geforderte Bewegung von in Ruhenden Flüssigkeiten Suspendierten Teilchen; von A. Einstein," *Ann. Phys.*, **17**, 549 (1905).

Holt, C. F., A. A. Boiarski, and H. E. Carlton, "The Gas Turbine Heat Exchanger in the Fluidized-Bed Combustor," *Int. Conf. on Fluidized Bed Combustion*, Philadelphia, **1**, 295 (1982).

Jost, W., *Diffusion in Solids, Liquids, Gases*, Academic Press, New York, 30 (1952).

Jovanovic, G. N., N. M. Catpovic, T. J. Fitzgerald, and O. Levenspiel, "The Mixing of Tracer Gas in Fluidized Beds of Large Particles," *Fluidization*, J. R. Grace and J. M. Matsen, eds., Plenum, New York, 325 (1980).

Kunii, D., and O. Levenspiel, *Fluidization Engineering*, Wiley, New York (1969).

LaNauze, R. D., "Fundamentals of Coal Combustion in Fluidized Beds," *Chem. Eng. Res. Des.*, **63**, 3 (1985).

Lee, Y. Y., A. F. Sarofim, and J. M. Beer, "Effects of Modes of Coal Feeding on Coal Volatile Release in Fluidized-Bed Combustors," *Fluidized Bed Combustion and Applied Technology*, R. G. Schwieger, ed., Hemisphere/McGraw-Hill, III-85 (1984).

Li, C. Z., M. C. Zhang, P. M. Walsh, J. M. Beer, and A. Dutta, "Measurements and Modelling of Oxygen Consumption in Fluidized-Bed Combustion," *Fluidized Bed Combustion and Applied Technology*, R. G. Schwieger, ed., Hemisphere/McGraw-Hill, II-25 (1984).

Ljungström, E. B., "In-Bed Oxygen Measurements in a Commercial-Size AFBC," *Int. Conf. on Fluidized Bed Combustion*, Houston, **2**, 853 (1985).

Minchener, A. J., D. C. Read, P. T. Sutcliffe, and J. Stringer, "The Use of Solid-State Electrochemical Probes for Characterization of Fluidized-Bed Environments," *Int. Conf. on Fluidized Bed Combustion*, Houston, **2**, 822 (1985).

Mori, S., and C. Y. Wen, "Estimation of Bubble Diameter in Gaseous Fluidized Beds," *AIChE J.*, **21**(1), 109 (1975).

Nienow, A. W., and T. Chiba, "Fluidization of Dissimilar Materials," *Fluidization*, 2nd ed., Ch. 10, J. F. Davidson, R. Clift and D. Harrison, eds., Academic Press, 369 (1985).

Nienow, A. W., P. N. Rowe, and T. Chiba, "Mixing and Segregation of a Small Proportion of Large Particles in Gas Fluidized Beds of Considerably Smaller Ones," *AIChE Symp. Ser.*, **74**(176), 45 (1978).

Park, D., O. Levenspiel, and T. J. Fitzgerald, "Plume Model for Large Particle Fluidized-Bed Combustor," *Fuel*, **60**, 295 (1981).

Pillai, K. K., "The Influence of Coal Type on Devolatilization and Combustion in Fluidized Beds," *J. Inst. Energy*, **54**, 142 (1981).

———, "A Schematic for Coal Devolatilization in Fluidized Bed Combustors," *J. Inst. Energy, 55(424), 132 (1982).*

Rowe, P. N., "Prediction of Bubble Size in a Gas Fluidized Bed," *Chem. Eng. Sci.*, **31**, 285 (1976).

Saari, D. P., and R. J. Davini, "Evaluation of Instruments for In-Bed Oxygen Measurements in a Fluidized-Bed Combustor," *Int. Conf. on Fluidized-Bed Combustion*, Philadelphia, **2**, 995 (1982).

Shi, Y., and L. T. Fan, "Lateral Mixing of Solids in Batch Gas-Solids Fluidized Beds," *Ind. Eng. Chem. Process Des Dev.*, **23**, 337 (1984).

Stubington, J. F., "The Role of Coal Volatiles in Fluidized Bed Combustion," *J. Inst. Energy*, **53**, 191 (1980).

Stubington, J. F., and J. F. Davidson, "Gas-Phase Combustion in Fluidized Beds," *AIChE J.*, **27**(1), 59 (1981).

Stubington, J. F., and Sumaryono, "Release of Volatiles from Large Coal Particles in a Hot Fluidized Bed," *Fuel*, **63**, 1013 (1984).

Stubington, J. F., and S. W. Chan, "Development of a 'Simulated' Coal Particle for the Study of Coal Volatiles Combustion in a Fluidized Bed," *Proc. CHEMECA 86*, Adelaide, Australia, 336 (1986).

Stubington, J. F., T. M. Linjewile, and G. D. Sergeant, "Devolatilization and Fragmentation of Large Coal Particles," *Int. Coal Sci. Conf.*, Maastricht, 833 (1987).

Stubington, J. F., and S. W. Chan, "Fluidized Bed Combustion of 'Simulated' Coal Volatiles," *Australian Coal Sci. Conf.*, Adelaide, Paper B3:4 (1988a).

Stubington, J. F., and S. W. Chan. "A Combined Oxygen/Bubble Probe for the Study of Fluidized-Bed Combustion of Volatiles," *Int. Symp. on Comb.*, The Combustion Institute, paper No. 47 (1989).

Stubington, J. F., and S. W. Chan, "Fluidized-Bed Combustion of Simulated Coal Volatiles," NERDDP end of grant report (NERDDP EG89/786) (1988b).

Turnbull, E., Ph.D. Diss., "Fluidized Combustion of Char and Volatiles from Coal," Univ. of Cambridge, U.K. (1983).

Walsh, P. M., A. Dutta, and J. M. Beér, "The Progress of Char Oxidation in Fluidized-Bed Combustion of a Bituminous Coal," *Coal Conf.*, Pittsburgh, 664 (1986).

Yates, J. G., M. MacGilliveray, and D. J. Cheesman, "Coal Devolatilization in Fluidized-Bed Combustors," *Chem. Eng. Sci.*, **35**, 2360 (1980).

Zhang, X., S. Wu, Y. Cao, and W. Dong, "Coal Devolatilization in Fluidized-Bed Combustors and the Distributor with Unequal Vent Area Rate," *Int. Conf. on Fluidized-Bed Combustion*, ASME, 1176 (1987).

Manuscript received Nov. 21, 1988, and revision received Sept. 12, 1989.